PLOS One

RESEARCH ARTICLE

Green synthesis, characterization, molecular simulation, and in vitro biomedical application of magnesium oxide nanoparticles

Samy Selim[1*], Mohamed K. Y. Soliman[2], Mohammed S. Almuhayawi[3], Mohammed H. Alruhaili[3,4], Hattan S. Gattan[5,4], Amna A. Saddiq[6], Nashwa Hagagy[7,8], Ashwag Jaman Alzahrani[6], Soad K. Al Jaouni[9], Salem S. Salem[2*]

1 Department of Clinical Laboratory Sciences, College of Applied Medical Sciences, Jouf University, Sakaka, Saudi Arabia, **2** Botany and Microbiology Department, Faculty of Science, Al-Azhar University, Nasr City, Cairo, Egypt, **3** Department of Clinical Microbiology and Immunology, Faculty of Medicine, King Abdulaziz University, Jeddah, Saudi Arabia, **4** Special Infectious Agents Unit, King Fahad Medical Research Center, King Abdulaziz University, Jeddah, Saudi Arabia, **5** Department of Medical Laboratory Sciences, Faculty of Applied Medical Sciences, King Abdulaziz University, Jeddah, Saudi Arabia, **6** Department of Biological Sciences, College of Science, University of Jeddah, Jeddah, Saudi Arabia, **7** Department of Biology, College of Science & Arts at Khulis, University of Jeddah, Jeddah,Saudi Arabia, **8** Botany and Microbiology Department, Faculty of Science, Suez Canal University, Ismailia, Egypt, **9** Department of Hematology/Oncology, Scientific Chair of Prophetic Medicine Application, Faculty of Medicine, King Abdulaziz University and Hospital, Jeddah, Saudi Arabia

* sabdulsalam@ju.edu.sa (SS); salemsalahsalem@azhar.edu.eg (SSS)

OPEN ACCESS

Citation: Selim S, Soliman MKY, Almuhayawi MS, Alruhaili MH, Gattan HS, Saddiq AA, et al. (2025) Green synthesis, characterization, molecular simulation, and in vitro biomedical application of magnesium oxide nanoparticles. PLoS One 20(9): e0332367. https://doi.org/10.1371/journal.pone.0332367

Editor: Balraj Baskaran, K Ramakrishnan College of Technology, INDIA

Received: October 28, 2024

Accepted: August 12, 2025

Published: September 17, 2025

Data availability statement: All relevant data are within the paper and its Supporting information files.

Funding: This work was funded by the Deanship of Graduate Studies and Scientific

Abstract

Microbial infections represent a major hazard to global public health, resulting in extensive morbidity and mortality across the globe. As a result, in the past 10 years, nanoparticles have drawn a lot of interest in their potential to manage microbial diseases. One of the few studies that has used a green and environmentally acceptable approach of producing magnesium oxide nanoparticles (MgONPs) was employed via using an extract from watermelon peels. UV–visible, FTIR, XRD, and TEM were used to comprehensively characterize the biosynthesized MgONPs. The synthetic MgONPs have a polycrystalline form with a median particle size of 6–17 nm, according on the characterization of the material. According to the antimicrobial results, MgONPs showed notable antimicrobial properties toward B. *subtitles, S. aureus, E. coli, P. aeruginosa*, and *C. albicans*, with an inhibition zone measuring 18.2 ± 0.36, 23.7 ± 0.4, 15.4 ± 0.25, 17.6 ± 0.56, and 16.3 ± 0.32 mm respectively. While the minimum inhibitory concentrations (MICs) varied from 50 to 200 μg/mL. MgONPs have successfully demonstrated antibiofilm potential versus MRSA. A molecular docking simulation was carried out to obtain a better understanding of the potential mechanism of MgO-NPs against the *S. aureus* strain. The results imply that the activity may be attributed to the dihydrofolate reductase (DHFR) with a varying degree, and the predominant interaction observed is the hydrophobic interaction with the residues' amino acids in the active site of the pocket in *S. aureus*. Furthermore, the DPPH

Research at Jouf University under grant No. (DGSSR-2025-FC-01007).

Competing interests: The authors have declared that no competing interests exist.

technique revealed that MgONPs had considerable antioxidant activity, with an IC_{50} of 223 µg/mL. Additionally, at a dosage of 62.5 µg/mL, MgONPs exhibit possible antiviral efficacy against HAV and HSV1, with proportions of 84.7 and 49.7%, respectively. Finally, the watermelon peel extract biosynthesized MgONPs exhibit antimicrobial, antibiofilm, antioxidant, and antiviral properties that show promise to be utilized in the biomedical field.

Introduction

Given that nanotechnology possesses so many uses in several scientific and technological domains, it has become a prominent subject of study recently [1,2]. It covers the formation of various types of nanoparticles (NPs) and how to use them in a range of industries, including biology, sensing, and catalysis [3]. Considering their remarkably high surface area compared to volume ratio, tiny particle size, changeable form, and high mechanical, optical, magnetic, and electrical qualities, among other attributes [4]. Nevertheless, the unique characteristics of a given NP are mostly determined by their synthesis method [5,6]. NPs may have produced in a variety of physical and chemical ways [7]. They need several hazardous chemical additions, high temperatures, vacuum conditions, and extremely complex instrumentation. However, the employment of many hazardous and reactive compounds in innovative chemical creation processes has also increased potential biological hazards to the ecosystem and the general populace. Significant effort has been devoted to an alternate and workable green synthesis method to produce numerous NPs to address these issues [8]. This preference arises because, compared to conventional chemical and physical techniques which often require hazardous substances and large amounts of energy, green synthesis is simpler, safer, more reliable, economical, and environmentally friendly [9–11]. The green or biosynthesis of NPs can be achieved using various plant materials, including roots, flowers, leaves, stems, bark, etc. [12,13]. The development of metal-based nanoparticles marks a significant advancement in nanotechnology, enabling the production of superior materials. Recently, researchers have successfully synthesized iron, silver, selenium, copper oxide, and gold nanoparticles using fruit and vegetable peels as well as their bagasse, which exhibit potent antibacterial and water-remediation properties [14,15]. The sustainable production of these nanomaterials depends on several factors, including the natural proportion of the metallic precursor, temperature, reaction duration, pH, and other reaction conditions [16]. Variations in these factors result in NPs with different sizes and morphologies, which greatly affect their physico-chemical as well as biological properties [17,18]. Metallic oxide nanoparticles (MNPs) are considered a significant group of widely used nanomaterials due to their unique chemical and physical-characteristics, as well as their many applications in biologica-medicine, food packaging, tissue engineering, catalysis, and environmental sciences [19,20]. Magnesium oxide nanoparticles (MgO-NPs), a type of metal oxide nanoparticle, have recently attracted considerable owing to their remarkable biomedical applications, biocompatibility, and exceptional stability under harsh-conditions [21,22].

MgO-NPs may readily engage with various biological-systems due to their beneficial physico-chemical properties, which include degree of ionicity, large surface-area, unique crystal structure, and oxygen deficiencies [23–25].Additionally, MgO-NPs have been explored as potential antifungal [26], antibacterial [27], antioxidant [28], anticancer [22] and antidiabetic agents [28]. Given the increasing prevalence of MgO-NPs in biomedicine, it is imperative to develop novel synthetic methods for their production. A thorough literature review reveals that the potential use of agricultural waste in the synthesis of MgO-NPs has not been extensively explored [29–31]. According to some studies, such waste could be converted into sustainable nanomaterials. The ideal biomass for cost-effective and environmentally friendly MgO-NPs synthesis would be a material with no competing beneficial uses. Watermelon peels, an abundant agricultural waste product, could serve as a viable source for this purpose.

This study aims to utilize watermelon peel extract (WPE) for synthesis of magnesium oxide nanoparticles. The synthesized MgO-NPs were characterized using TEM, XRD, UV-Vis spectroscopy, and FT-IR. Furthermore, their antibacterial, antibiofilm, antioxidant, and antiviral properties were evaluated (Fig 1).

Materials and methods

Materials

Magnesium nitrate hexahydrate ($Mg(NO_3)_2{\cdot}6H_2O$, ≥ 99.0%, Sigma-Aldrich, Cairo, Egypt. Sodium hydroxide (NaOH, ≥ 98%, pellets, Sigma-Aldrich, Cairo, Egypt). All media used for biological activities (antibacterial and antibiofilm) from Oxoid Dist., Cairo, Egypt. DPPH (2,2-diphenyl-1-picrylhydrazyl, ≥ 95%, Sigma D9132). In addition, the reagents or biological medium don't need to be purified before use [32].

Watermelon peels extract preparation

The watermelon was purchased from Carrefour market (30.174352611096854, 31.476022880013325) at Obour City, Qalyubia Governorate, Egypt. The watermelon peel (WP) was cleansed with thoroughly distilled water many times, and the same technique was used to establish the extract as in a previous study with a few little adjustments [33]. Next, the peel (the white portion alone) was sliced into little pieces (about 1 cm) and placed in 200.0 g with 1 L of d. water. Following

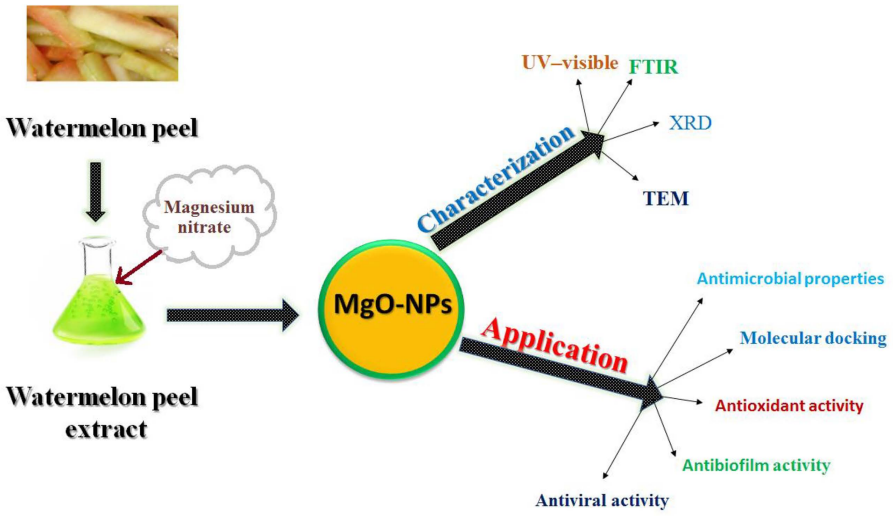

Fig 1. A schematic-diagram illustrating the production, characterisation, and applications of MgO-NPs synthesized by WP extract.

https://doi.org/10.1371/journal.pone.0332367.g001

utilizing a magnetic stirrer to continuously agitate the mixture for 10 min, employing Whatman no. 1 filter paper, WPE had been cooled, collected into an uncontaminated bottle, then kept at 4°C as long as required.

Biosynthesis of MgO-NPs

Following the last study with a few minor adjustments, the Sharma et al. [34] technique was ensued in order to generate MgO-NPs. In summary, 50 mL of freshly prepared magnesium nitrate (1.0 mM) solution was combined with Fifty mL of watery WP extract. The mixture was then mixed with ten milliliters of drops of added sodium hydroxide (1.0 M) at 80°C. For four h., the solution was continuously stirred at 500 rpm using a magnetic-stirrer. The colour transformation from pale yellow to brownish served as an indication to start generating nanoparticles. Next, the produced MgO-NPs were calcined for 3-h at 200°C to produce the dry MgO-NPs and the resulting powder was maintained in the dark for further-investigation.

Characterization of generated MgO-NPs

A variety of modern analytical techniques were employed to characterize the biosynthesized MgO-NPs. Initially, a shift in colour was used to visually observe the creation of MgO-NPs. Employing a spectrophotometer (JENWAY 6305 Spectrophotometer), UV-Vis spectroscopy, the colour change resulting from the synthesis of NPs exhibiting a wavelength of 200–700 nm [35]. The structural features of the generated MgO-NPs were investigated utilizing a TEM (JEOL- 1010 -Japan). After adding a drop of the MgO-NPs onto the C-coated Cu- grid, it was let dry out until being set on a holder. Furthermore, it was allowed to image the specimen that was gathered. With the use of FT-IR spectroscopy (Agilent system Cary 660 FT-IR model), the goals of the functional groups in charge of the reduction, capping, and stability of MgO-NPs were evaluated. The 400–4000 cm^{-1} region of FT-IR spectra was used to analyze the materials [36]. Furthermore, the crystalline form of biosynthesized MgO-NPs was examined using the X-ray diffractometer X′ Pert Pro (Philips, Eindhoven, the Netherlands) and designs created by XRD. The range of values for 2θ was 4^{o} to 80^{o} on average. Cu Ka radiation that had been Ni-filtered was the source of the X-rays. A 40 kV voltage and a 30 mA current were present, respectively. WP extract's median size of MgO-NPs was determined by applying the Debye-Scherrer equation [37].

Antimicrobial properties of MgO NPs

Utilizing the agar well diffusion technique, the antibacterial activity of the MgO-NPs was assessed toward *Pseudomonas aeruginosa* ATCC 9022, *Escherichia coli* ATCC 8739, *Bacillus subtilis* ATCC 6633, *Staphylococcus aureus* ATCC 6538, and *Candida albicans* ATCC 10231. Muller Hinton agar (MHA) and tryptic soy agar (TSA) serve as the mediums employed for observing the growth of the microbial strains (Oxoid, USA). After a day, the suspension of microbes was added to autoclaved medium that had an average density of half of the McFarland standard. After that, they were divided equally across the Petri dishes. With the use of a sterile cork-borer, an 8 mm hole was made. Next, 100 µl of the MgO-NPs (1000 µg/ml) had been added to the well, and it was incubated at 37°C for 24 h. In the same way, WP extract and magnesium nitrate were used as negative control tests. Amoxicillin (1000 µg/ml) functioned as the positive- control for bacterial tests, while Fluconazole (1000 µg/ml) was used as the positive-control for fungal test. Using a digital caliper, the region of suppression was determined after incubation [38]. The diameters of the zones were expressed in mm. The outcome was recorded in compliance with CLSI criteria [39].

The MIC of MgO-NPs against pathogenic microorganisms was determined using the broth microdilution method [36]. Different amounts of MgO-NPs have been generated, ranging from 800 µg/mL to 12.50 µg/mL. Sterilized MTP wells were filled with MgO-NPs to be evaluated at various concentrations after 100.0 µL of double-strength Mueller hinton (MH) broth was supplied. A microbial-suspension of cells (20 µL) matching the 0.5 McFarland standard has been added, excluding the negative and positive control wells. For twenty-four hours, the plates are incubated at 37°C. The MIC was determined in accordance with the Clinical and Laboratory-Standards Institute (CLSI) guidelines using a microplate-reader

(STAT-FAX, USA) and the least quantity of samples that suppressed the test pathogens in a way that was analogous to negative as well as positive controls [40].

Anti-Biofilm activity of biosynthesized MgO-NPs

The microtiter plate (MTP) method was employed to assess the anti-biofilm activity of MgO-NPs against *S. aureus* MRSA, a clinical strain renowned for its strong biofilm-forming capacity. A few changes were made to the biofilm- experiment from the last study. In summary, MgO-NPs were introduced in varying quantities to MTP, including TSB Media that were enriched with 1% glucose. The experimental microorganism was set up on MTP over 48 h at 37.0°C after being diluted 1:100 in TSB. Following the incubation time, the development density (OD at 620nm) had been determined before removing the planktonic cells onto the dishes. Subsequently, wells were gently washed 3-times with phosphate-buffered saline (PBS) to preserve intact biofilms. Biofilms were fixed with 200 µL of 95% methanol for 10 min, followed by staining with 0.3% crystal violet (200 µL/well) for 20 min at room-temperature. Excess stains were removed by washing with distilled-water, and biofilm-associated dye was solubilized with 30.0% acetic Acid for quantification. Employing a microplate-reader (STAT-FAX-USA) set to O.D. at 540 nm, the absorbance was obtained. By comparing to control wells, the results were confirmed [41].

Molecular docking

The Molecular Operating -Environment (MOE) version MOE- 2019.0102 was utilized to carry out the molecular docking simulation procedure for MgO-NPs. Target receptor dihydrofolate reductase's 3D structure (PDB: 2w9h) (Fig 2) was obtained from the protein -data bank using the following link: https://www.rcsb.org/structure/2veg (last accessed 4/10/2024). By applying the previously described method [42], just one chain (chain- A) was needed to build the receptor's active site. The construction of dihydrofolate reductase (PDB: 2w9h) involved the generation of an active site through the selection of (chain A) and subsequent generation in accordance with standard protocol. The docking process was completed using triangle- matcher placement, London-dG, and GBVI/WSAdG- as Rescoring-1 and 2, respectively. In addition, Forcefield was used for post-placement refinement. The docking attitude exhibited the most binding energy, with a negative value. In addition, the MgO-NPs structure was created using the identical procedure as previously reported [42].

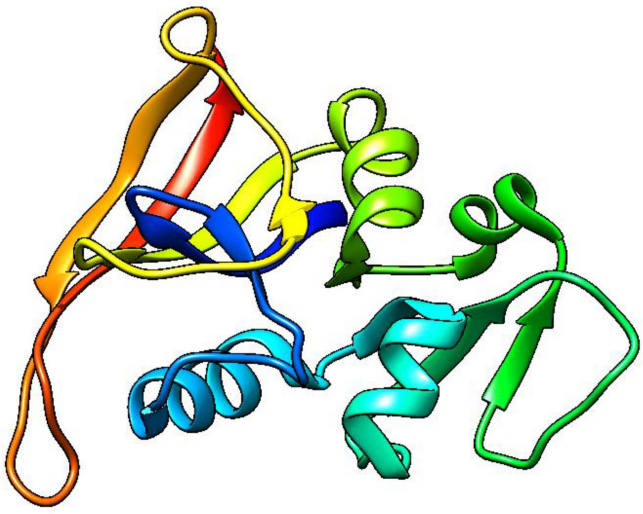

Fig 2. 3D crystallography of the DHFR enzyme obtained from protein data bank.

https://doi.org/10.1371/journal.pone.0332367.g002

Antioxidant activity of biosynthesized MgO-NPs

To test MgO-NPs' antioxidant properties, the DPPH technique was applied [43]. The ability of bio-synthesized MgO-NPs to scavenge DPPH radicals was tested at various doses (1000 to 7.81 µg/mL). The antioxidant capability of ascorbic acid (AA) was assessed using the methodology of Almuhayawi et al., [44], and the subsequent equation has been employed to compute the DPPH- scavenging activity (%) for different quantities of MgO-NPs.

$$\text{DPPH} - \text{scavenging activity}\ (\%) = \text{A1}) - \text{A2})/\ \text{A1})\ \times 100$$

A1): Absorbance of control, A2): Absorbance of test

Antiviral activity of biosynthesized MgO-NPs

To determine (MNTC of the synthesized MgO NPs, the particles were added to a 96-well plate containing standard Vero cells (ATCC CCL-81, Science Way Co., Cairo, Egypt) as host cells. The MTT assay was then used to calculate the MNTC. A confluent monolayer of Vero cells was prepared by seeding 10^4 cells/well in 100.0 µL growth medium, followed by incubation in a 5% CO_2 incubator at 37°C for 24 h. After incubation, the growth medium was removed, and the cells were treated with MgO-NPs at concentrations ranging from 1000 to 31.25 µg/mL. Untreated cells served as the negative control in the triplicate tests of MgO-NPs dissolved in DMSO at each dose. In a 5% CO_2 condition, treated plates were left to stand for 48 h at 37.0°C. After incubation, each well received 20 µL of MTT- solution, which was agitated for 5 min at 150.0 rpm and then incubated for 5 h at 37°C with CO_2. Following supernatant removal, 200 µL of DMSO was added to each well to dissolve the formed formazan crystals. The absorbance was subsequently recorded at 570 nm using a microplate ELISA reader. The MNTC was determined by plotting the relationship between MgO-NPs concentrations and cell viability percentages.

The antiviral efficacy of MgO-NPs against the herpes simplex-virus (HSV-1) and hepatitis A- virus (HAV) was evaluated. A confluent monolayer of Vero cells was prepared, and a viral-suspension was incubated with MgO NPs (1:1 (v/v) for 1 h at 35.0 ± 2°C. Then, 100.0 µL of the virus-NP mixture was added to each well. Untreated Vero cells (non-infected) served as the control. The plate was shaken at 150.0 rpm for 5 min and incubated overnight at 37.0°C with 5% CO_2. Cell viability was assessed by measuring formazan crystal absorbance after adding MTT solution. In the same way, Acyclovir and Amentadine served as the positive controls for HSV-1 and HAV tests, respectively. By contrasting the optical density (OD) values of live infected cells with those of uninfected controls, the effectiveness of the antiviral treatment was evaluated [45].

Statistical analysis

Three replications' means and the standard deviation (SD) were calculated for each of the outcomes, and the data thereafter underwent an analysis of difference utilizing one-Way and two-Way ANOvA at Graph Pad prism-version 8.0.2.(p-value < 0.05 (*), p-value < 0.01 (**), p-value < 0.001(***), p-value < 0.0001(****))

Results and discussion

Biosynthesis of MgO-NPs using WP extract

Fruit peels, typically discarded as waste, are an excellent-source of phytochemicals that play a crucial role in nanomaterial synthesis. When plant organ extracts were used for nanoparticle production, varied results were observed. In our study, MgO-NPs formed after 4 hours of incubation, with visual inspection revealing a steadily increasing synthesis rate. Following nanoparticle formation, the solution colour changed from clear to yellowish-brown, indicating successful synthesis. The watermelon peel (WP) extract served as both a reducing and capping agent, enhancing the colloidal stability of the NPs. Even at low concentrations, the biomolecules present in the extract not only reduced the number of metal ions required for nanoparticle formation but also prevented aggregation of the synthesized NPs [46]. The optical properties of the colloidal

nanoparticle solution varied depending on the particle size and shape, primarily due to surface-plasmon-resonance (SPR). Key phytochemicals in fruit peels—such as aldehydes, flavones, amides, terpenoids, and sugars—facilitate bioreduction and NP stabilization [47].

Characterization of biosynthesized MgO-NPs

Research has confirmed that the phytochemical components present in watermelon peel (WP) extract facilitate the synthesis of MgO-NPs. When the WP extract reduced magnesium ions in solution, MgO-NPs were formed. The first observable evidence of successful biosynthesis occurred when the mixture of aqueous WP extract and magnesium nitrate salt changed colour from light yellow to yellowish-brown. This colour transformation resulted from surface plasmon resonance (SPR), a characteristic optical property of MgO-NPs, with absorption maxima (λ_{max}) in the 260–300 nm visible range [48]. The generated nanoparticles' dimensions, morphologies, nature, excellent dispersion, particle-to-particle separation, and external medium all had a substantial impact on the SPR absorbance [49]. According to Jeevanandam et al., the generated MgO-NPs appear to be lower in diameter at SPR frequencies not more than 300 nm; still, the degree of anisotropy increases for SPR greater than 300 nm [50]. The present investigation evaluated the optical- properties of MgO-NPs developed via WP extract mediated at wavelengths spanning from 200 to 700 nm. MgO-NPs UV-Vis spectra showed the existence of nanoscale particles, with a resonance band at 275 nm (Fig 3). The finding is displayed as associated with other researchers [51,52]. The most noticeable bands of MgO-NPs derived from *Tecoma stans* (L.) and *Rosmarinus ofcinalis* L were found at 282, and 250 nm, respectively, according to these investigations [51,52]. Furthermore, MgO-NPs made chemically had a measurable absorbance band at 290 nm [53].

Fourier-transform infrared (FTR)-spectroscopy (4000–400 cm^{-1}) revealed that the WP extract performed two responsibilities in the process of MgO-NPs, modelling as both a capping agent and reducing agent for the participating functional groupings. The FTIR spectrum of the biosynthesized MgO-NPs exhibited characteristic absorption bands at 3406 cm^{-1} O–H stretching, 2354 cm^{-1} and 2345 cm^{-1} C–H vibrations, 1641 cm^{-1} C = C, *cis* configuration, 1423 cm^{-1} and 1384 cm^{-1} C–O

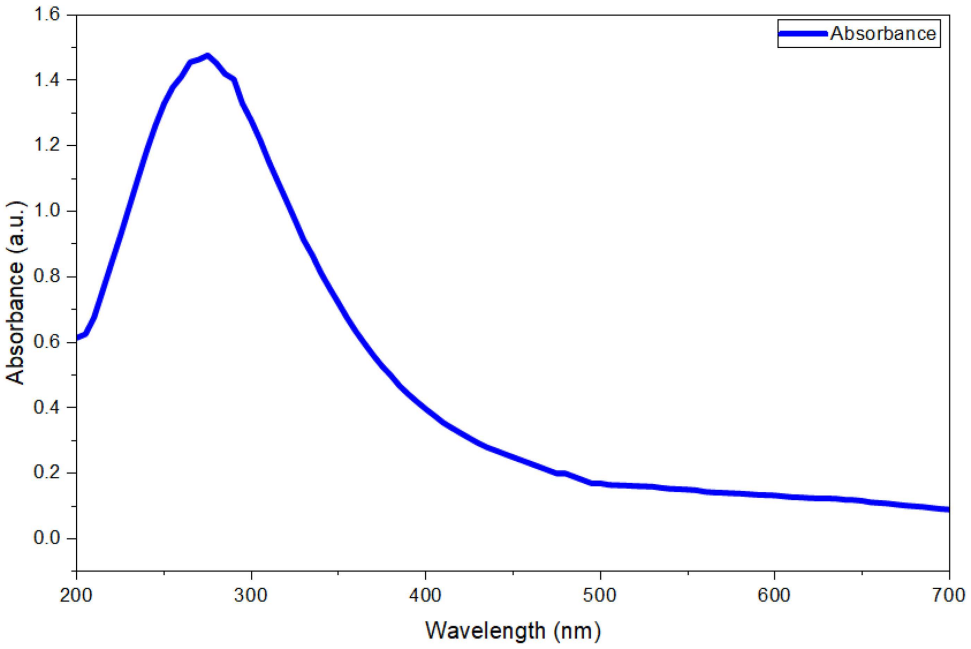

Fig 3. UV-vis spectrum of biosynthesis MgONPs.

https://doi.org/10.1371/journal.pone.0332367.g003

bonds, 1174 cm^{-1} and 1100 cm^{-1} flavonoids/tannins 616 cm^{-1}, 487 cm^{-1}, and 405 cm^{-1} Mg–O vibrations (Fig 4). These bands confirmed the presence of bioactive metabolites phenolics, carbohydrates, flavonoids, and tannins adsorbed on the NP surface [54]. The stability and formation of MgO-NPs depended on these functional molecules. Additionally, two distinct peaks at 635 cm^{1} and 495 cm^{1} were attributed to Mg–O vibrational modes, confirming MgO-NPs formation [55]. This finding aligns with previous reports identifying the 437–677 cm^{-1} range as characteristic of MgO-NPs synthesis [56].

The X-ray Diffraction (XRD) analysis confirmed both the crystalline-structure and phase purity of the biosynthesized MgO-NPs. The diffractogram (Fig 5) showed distinct diffraction peaks, verifying the crystalline-nature of MgO-NPs. The diffraction pattern revealed well-defined reflection of planes and a cubic crystal structure. The detected peaks confirmed the high-purity of the synthesized MgO-NPs, as they corresponded exclusively to the cubic phase of MgO without any secondary phase impurities. Five distinctive peaks were seen at 2θ values of 37.14°, 42.71°, 62.66°, 77.29°, and 78.46°, which were linked to the (111), (200), (220, (311, and (222) reflection planes, respectively. Additional peaks at 36.5° and 75.8° (corresponding to (111) and (311) planes) indicated the existence of trace levels of $Mg(OH)_2$. The broadening of peaks at (200), (220), and (222) suggested the formation of smallnanosized cubic MgO-NPs [57]. This XRD pattern was consistent with previous reports of green-synthesized MgO-NPs using various bioactive compounds [58,59].

The dimensions and form of NPs are often connected to their activity, since their performance increases progressively as the size decreases. The produced MgO-NPs' size formation and surface structural characteristics were examined using HR-TEM. In line with other research, the HR-TEM micrograph of MgO-NPs (Fig 6) clearly showed the spherical form of biosynthesized MgO-NPs [60]. Using a TEM at 100 nm, the generated MgO-NPs' nanometer size ranged from 6 to 17 nm. The properties of metabolites, including proteins and enzymes, in forming and altering the morphologies of specific-NPs, such as circular, cubic, and hexagonal, along with rods, are the main problems that require immediate attention and more research [61].

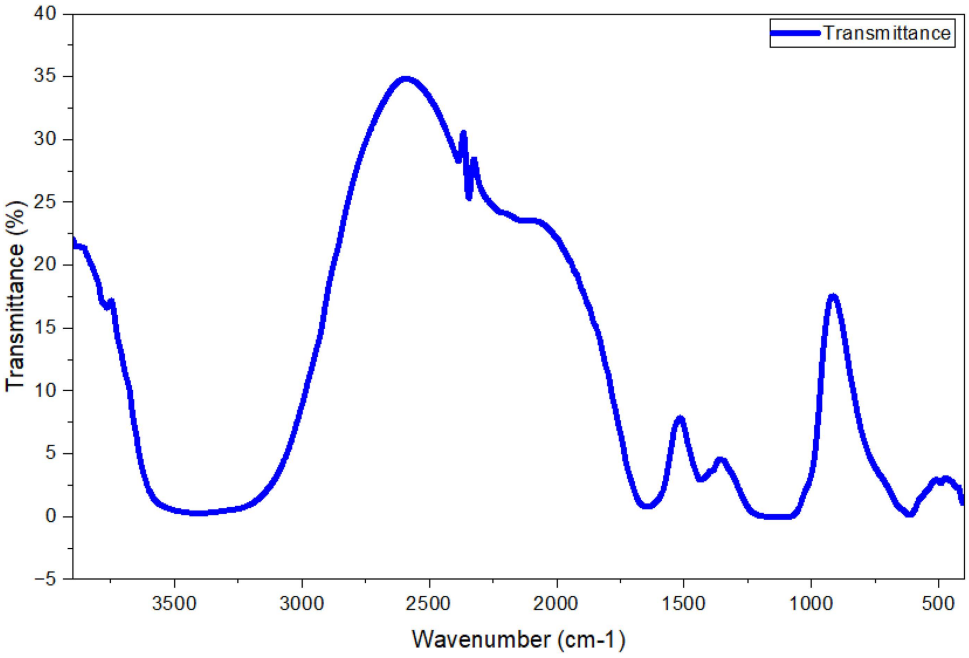

Fig 4. FT-IR spectra of biosynthesized MgONPs.

https://doi.org/10.1371/journal.pone.0332367.g004

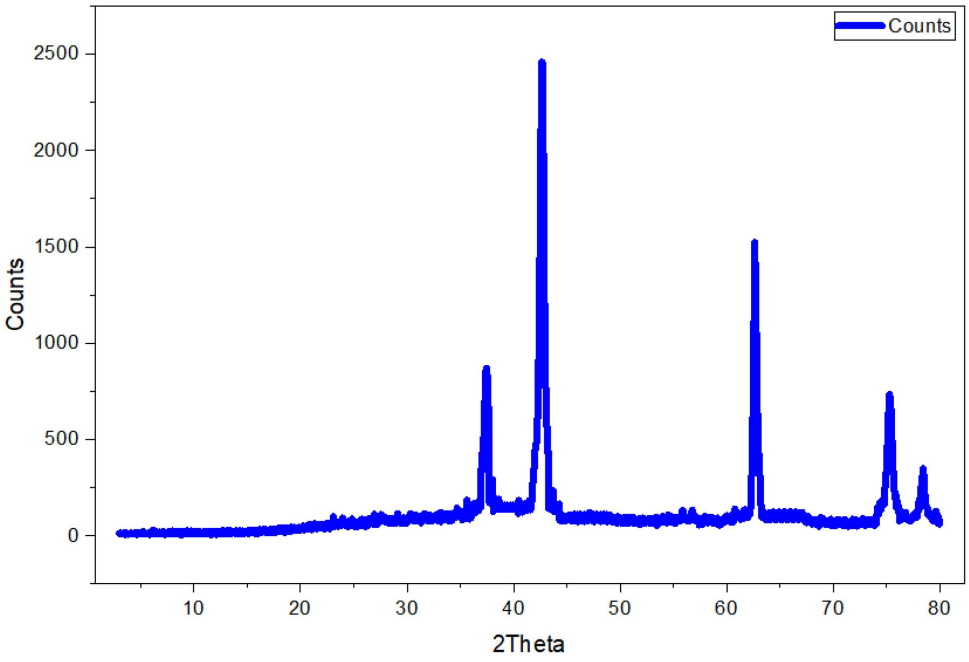

Fig 5. XRD analysis of biosynthesized MgONPs.

https://doi.org/10.1371/journal.pone.0332367.g005

Antimicrobial effectiveness of Biosynthesized MgO-NPs

Antimicrobial resistance (AMR) remains a major challenge in clinical infectious disease management. In accordance with the standards of the Clinical and Laboratory Standards-Institute (CLSI), the antibacterial activity of biosynthesised MgO-NPs was assessed using the agar diffusion technique. Inhibition zone diameters (mm) were measured to assess antimicrobial efficacy. As shown in Fig 7, the MgO-NPs exhibited significant antimicrobial activity, evident by clear inhibition zones. At 1000 µg/mL, the NPs demonstrated strong activity against *Bacillus subtilis* (18.2 ± 0.36 mm) and *Staphylococcus aureus* (23.7 ± 0.4 mm) (S1 Table). The lowest activity was observed against *Escherichia coli* (15.4 ± 0.25 mm) and *Candida albicans* (16.3 ± 0.32 mm). In contrast, *Pseudomonas aeruginosa* showed moderate susceptibility (17.6 ± 0.56 mm). These results may be attributed to the small size of MgO-NPs (32–39 nm), which has been previously reported to enhance antimicrobial effects against Gram-negative bacteria [60]. Notably, MgO-NPs synthesized using *Psidium guajava* leaves have demonstrated potent bactericidal properties [62]. Yoon et al. [63] and Das et al. [64] similarly reported that higher MgO-NPs concentrations increased antibacterial efficacy, particularly against *E. coli*, in a dose-dependent manner. The MIC values of MgO-NPs were determined as follows, 100 µg/mL for *B subtilis* and *P aeruginosa,* 200 µg/mL for *Ecoli* and *C albicans* and finally 50 µg/mL for *S aureus.* The antibacterial effect of MgO-NPs arises from the attraction between Mg^{2+} ions and the negatively charged bacterial cell surface, which causes damage to the cell wall, leads to protein malfunction, and results in cell death [65]. Adsorption of Mg^{2+} ions to membrane proteins, causing proton pump dysfunction and loss of membrane integrity [66]. Intracellular penetration of MgO-NPs, resulting in ATP depletion, reactive oxygen-species (ROS) generation, DNA/protein damage and membrane leakage [67]. Additionally, Sawai et al. [68] proposed that MgO-NPs adsorb water molecules, forming an alkaline surface layer (high pH) that damages bacterial membranes and induces cell death.

Anti-biofilm of Biosynthesized MgO-NPs

Biofilms are microbial communities that form surface-adherent structures, significantly enhancing microbial resistance to antimicrobial treatments [69]. These complex matrices consist of proteins, fibrin, and polysaccharides [70]. Notably,

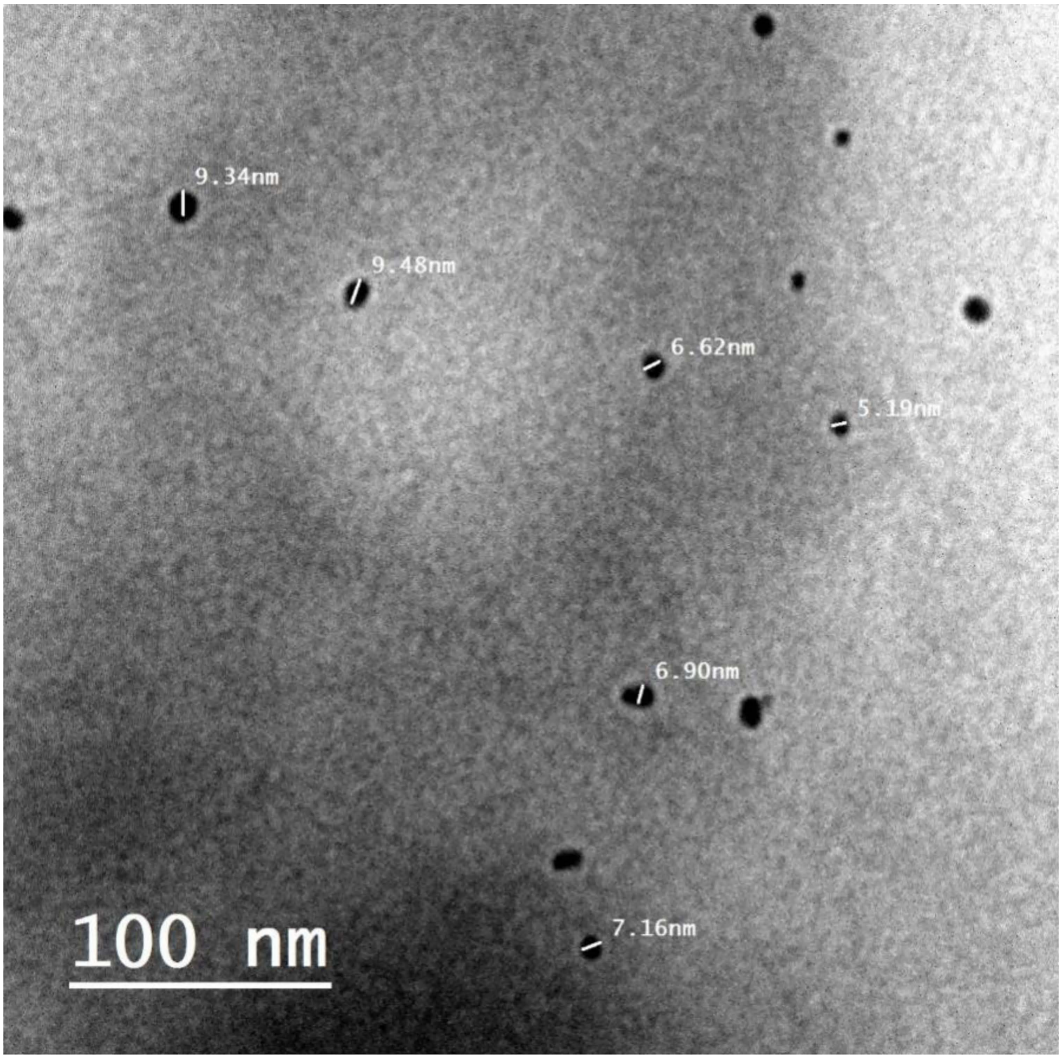

Fig 6. TEM image of the biosynthesized MgONPs.

https://doi.org/10.1371/journal.pone.0332367.g006

antibiotics effective against planktonic bacteria are often 10−1000 times less potent against bacterial biofilms [71]. In this study, MgO-NPs demonstrated dose-dependent antibiofilm activity against MRSA (S2 Table). The inhibition rates were 67.1% at 200 µg/mL, 50.9% at 100 µg/mL, 38.1% at 50 µg/mL, 22.2% at 25 µg/mL and 4.3% at 3.12 µg/mL (Fig 8). Light microscopy confirmed biofilm disruption, showing dissolution of microcolonies across all tested concentrations (200–3.12 µg/mL) (Fig 9). These findings align with Khan et al.'s results using the crystal violet assay [72]. MgO-NPs were more effective at preventing biofilm formation than eradicating established biofilms [73]. Compared to ciprofloxacin, MgO-NPs showed superior antibiofilm activity against *P. aeruginosa*, *S pyogenes* and *S epidermidis* [74]. Biofilm inhibition concentrations were sub-MIC doses (0.5 × MIC) significantly reduced mature biofilms for *S. aureus* 500 µg/mL, *Klebsiella pneumoniae* 125.0 µg/mL and *E. coli*: 250 µg/mL [75]. Low concentrations (10 µg/mL) effectively prevented *S. aureus* biofilm formation [76]. Smaller MgO-NPs (8 nm) showed enhanced inhibition against *S aureus* and *Ecoli* biofilms [77].

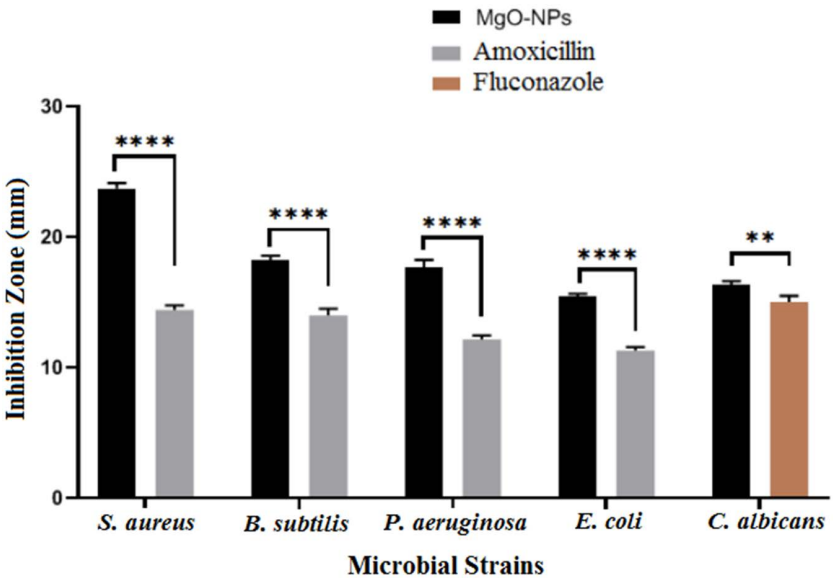

Fig 7. Antimicrobial properties of MgONPs versus different microbial strains.

https://doi.org/10.1371/journal.pone.0332367.g007

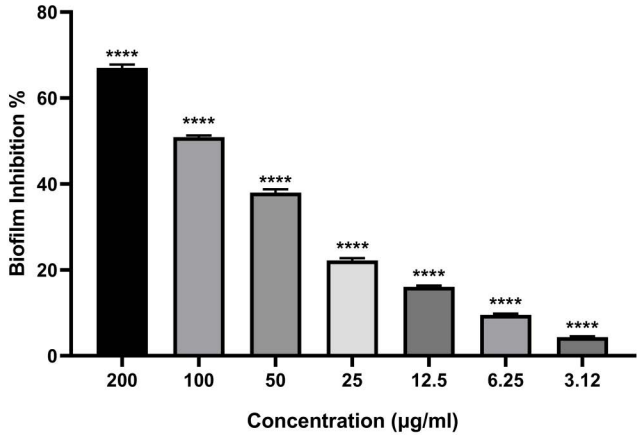

Fig 8. Antibiofilm activity of biosynthesized MgONPs toward MRSA at varying doses.

https://doi.org/10.1371/journal.pone.0332367.g008

Docking simulation

Molecular docking- simulation is a powerful computational tool for predicting the 3D structure of protein-ligand-complexes and analyzing their interaction mechanisms [78]. This technique also provides insights into the potential modes of action and biological responses of nanomaterials. In this study, we performed docking simulations of MgO-NPs with the active site of DHFR (PDB: 2W9H) from *Staphylococcus aureus* (Fig 1). Finding out how specific enzymes interacted with MgO-NPs was the aim of the study, which aimed to discover potential targets for antibacterial action. Initially, the DHFR (PDB: 2w9h) and the co-crystallized ligand's root mean square-deviation (RMSD) values were determined. They were 0.7813 and 0.9317 Å, respectively. The dihydrofolate reductase (DHFR) (PDB: 2W9h) was shown to display hydrophobic contact inside the active site of the MgO-NPs with various amino acid residues, including Tyr109 and Ser135 (Fig 10), and binding

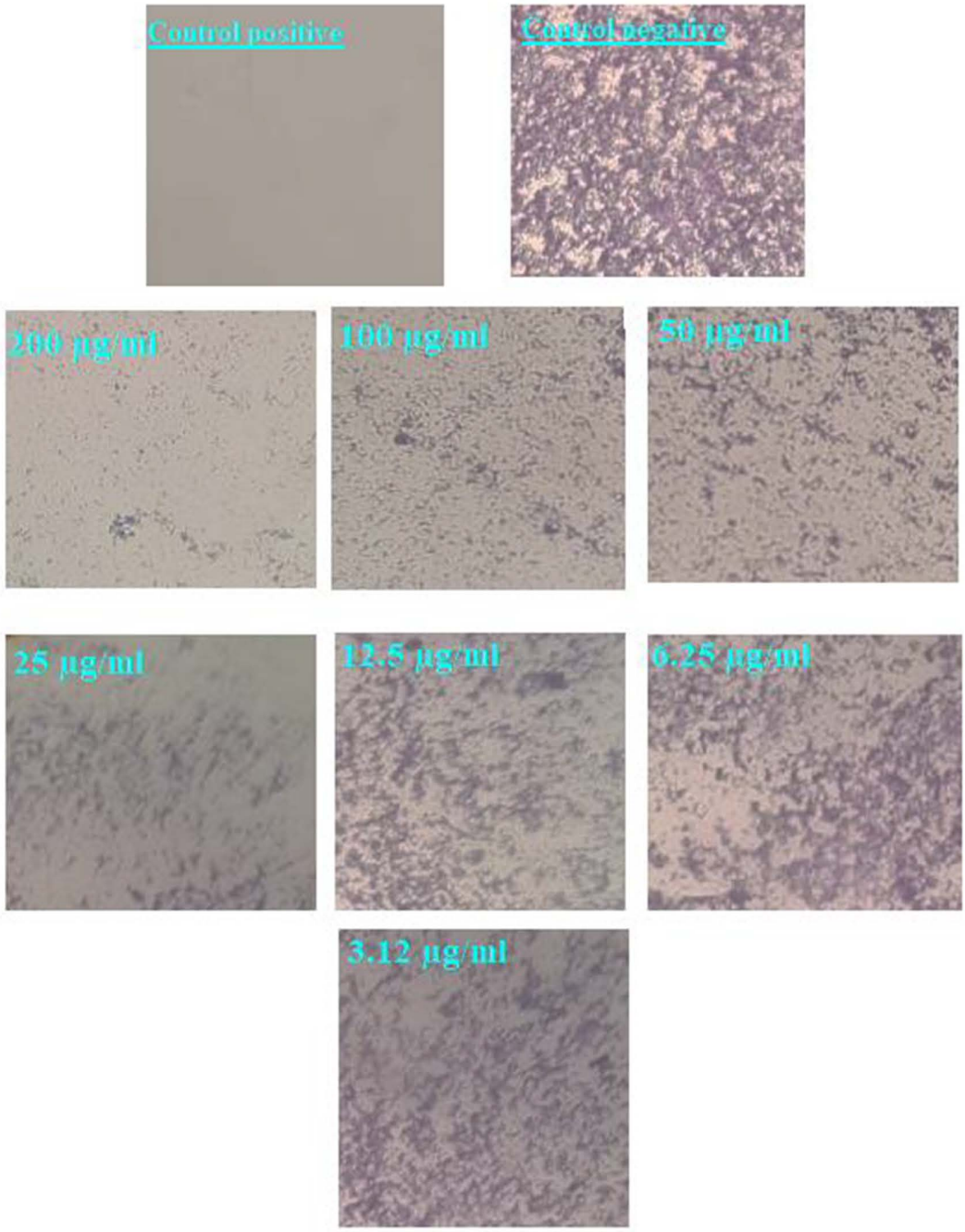

Fig 9. Light-inverted microscopy pictures of *S. aureus* biofilms cultivated in different MgONPs doses.

https://doi.org/10.1371/journal.pone.0332367.g009

energy S = −3.3015 kcal/mol. We can state that MgO-NPs demonstrate their antibacterial activity through the inhibition of dihydroorotase synthase. However, the binding energy suggests that MgO-NPs favour DHFR more, and their activity is indicated by hydrophobic-interactions in the pocket containing the active site, which is located less than 2.7 Å away. The effectiveness and binding affinity of the MgONPs with the *Staphylococcus aureus* DHFR enzyme were assessed, along

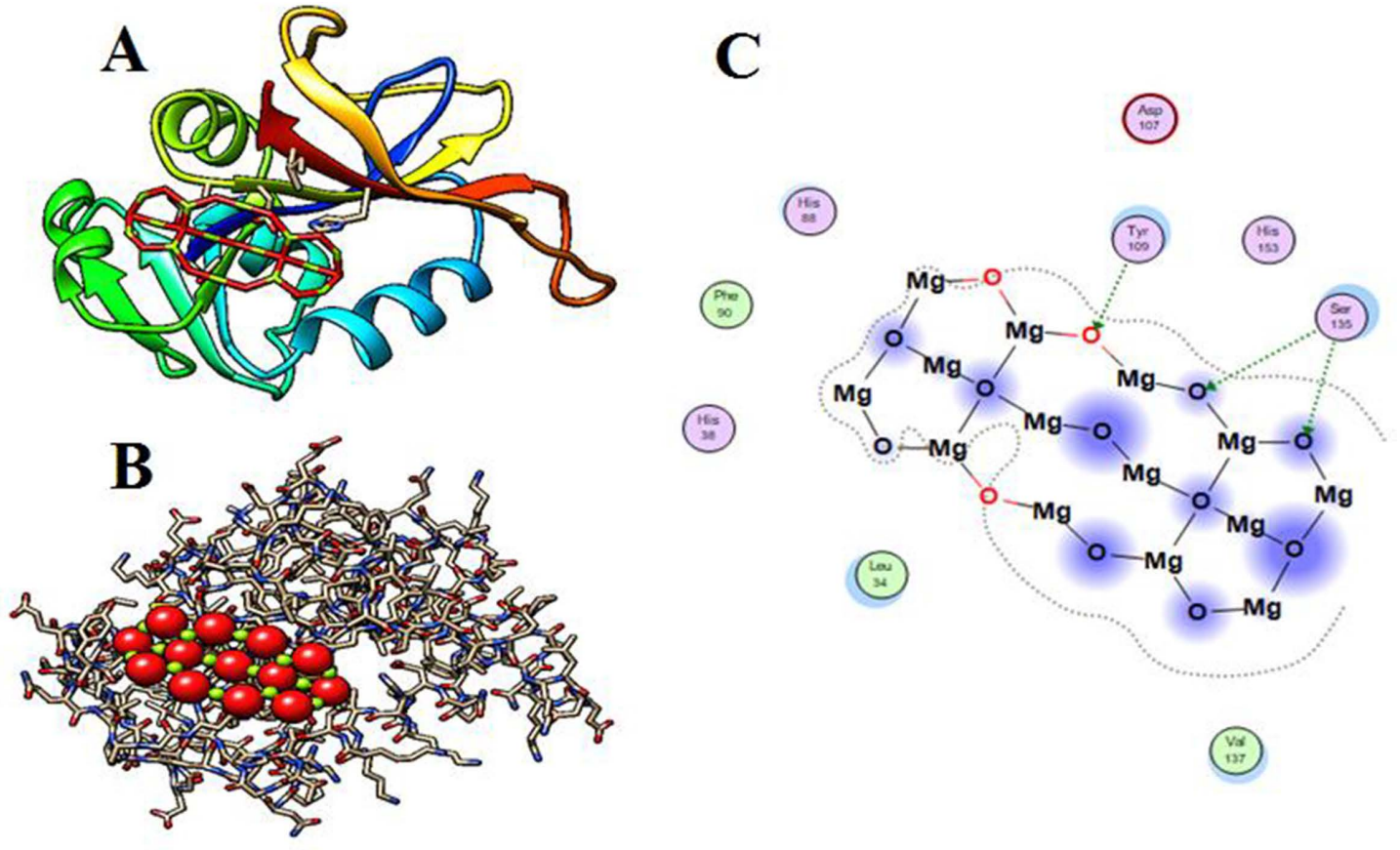

Fig 10. Structural interaction of MgO-NPs within the active site of dihydrofolate reductase (DHFR) (PDB ID: 2W9H). (A & B) 3D representations showing the binding mode of MgO-NPs within the DHFR active site, highlighting interactions with surrounding amino acid residues. (C) 2D interaction diagram illustrating the binding of MgO-NPs within the active pocket and their interactions with key amino acids.

https://doi.org/10.1371/journal.pone.0332367.g010

with the postulated method of binding to bacterial cells [79]. The most important enzyme for the bacterial species' survival is DHFR. It is necessary for cell development and proliferation and is extensively expressed in bacterial species. It is hypothesised that interactions between nanoparticles and this enzyme prevent DNA replication in this species [80]. Consequently, antibacterial medications in synthetic materials may exert their effects by forming favorable interactions with the amino acid residues of target enzymes.

Antioxidant activity

Fig 11 presents the antioxidant potential of MgO-NPs evaluated across a range of concentrations.UV-Vis spectroscopic analysis revealed distinct absorbance peaks at 517 nm, corresponding to DPPH radical scavenging activity. The scavenging efficiency increased proportionally with NP concentration, showing values of 75.8, 63.6, 52.3, 40.3, 32.1, 23.2, and 10.5% from 1000–15.63 µg/mL, correspondingly (S3 Table), are the percentages of DPPH scavenging of MgO-NPs at the highest doses and the IC50 of MgONPs was recorded at 223 µg/mL. The antioxidant mechanism involves electron transfer from MgO-NPs to DPPH radicals, converting the solution from purple to yellow, which confirms the strong antioxidant capacity of the synthesized NPs [81]. The enhanced antioxidant-properties of MgO_NPs can be attributed by the existence of additional flavonoids as well as phenolics as capping on the outer layer of the magnesium oxide NPs

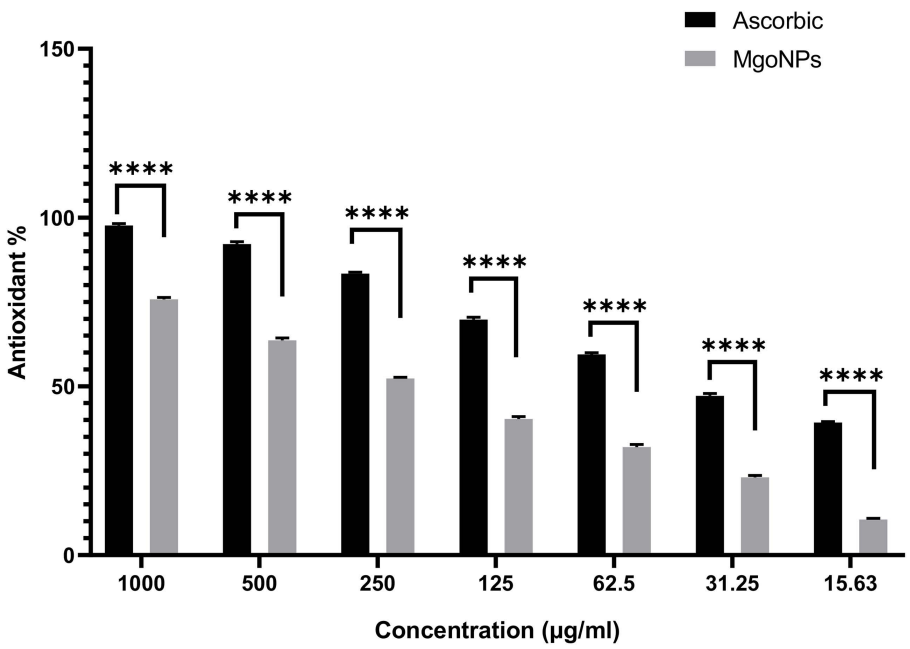

Fig 11. Antioxidant capability of biosynthesized MgONPs at varies concentrations.

https://doi.org/10.1371/journal.pone.0332367.g011

derived from extract [82]. Using a DPPH method, the antioxidant activity of magnesium oxide nanoparticles generated by *Clitoria ternatea* has been assessed. It was discovered that at a dose of 150 mg/ml, the biologically produced MgO-NPs' DPPH activity reach to 65% [83]. Using the DPPH test, Dobrucka et al. also investigated the antioxidant activity of produced MgO-NPs and discovered that they were antioxidants [84]. Additionally, free radicals such H_2O_2, O_2^-, and OH• as well as reactive-oxygen species (ROS) may be produced by NPs. Highly reactive substances called free radicals and ROS produce intense oxidative stress inside cells, which damages DNA, destroys proteins, and eventually results in cell death [85]. Most ROS are transformed into hydroxyl radicals [86]. Metal catalysts can decompose superoxide (O_2^-) and hydrogen-peroxide (H_2O_2), a process that generates hydroxy-radicals (•OH) [87]. This reactivity stems from the unpaired electrons in certain metals, which facilitate single electron transfer reactions. When hydroxyl radicals interact with DNA's sugar backbone, they abstract hydrogen atoms from each carbon, forming carbon-centered sugar radicals. These reactive intermediates subsequently cause base-free sites, DNA strand breaks and modified sugar products [88]. Biologically synthesized nanoparticles exhibit superior antioxidant capacity compared to those produced through chemical or physical methods. This enhancement is attributed to plant-derived capping agents, which consist of alkaloids, polysaccharides, flavonoids and phenolic compounds. These phytochemicals synergistically enhance the nanoparticles' antioxidant potential [89].

Antiviral Assessment of Biosynthesized MgO-NPs

This study assessed the antiviral effectiveness of MgO-NPs biosynthesized using WPE against hepatitis A-virus (HAV) and herpes simplex-virus 1 (HSV-1) (S4 Table). The cytotoxic potential of MgO-NPs was first examined using normal Vero cell lines, revealing a maximum non-toxic concentration (MNTC) of 62.5 µg/mL. Using the MTT antiviral assay, we demonstrated that Vero cell viability improved when treated with green-synthesized MgO-NPs in virus-infected cultures, compared to virus-only controls. Data analysis showed these biogenic MgO-NPs exhibited 84.7% antiviral activity against HAV and 49.7% against HSV-1 (Figs 12 and 13). It seems that there are several different ways that nanoparticles may break

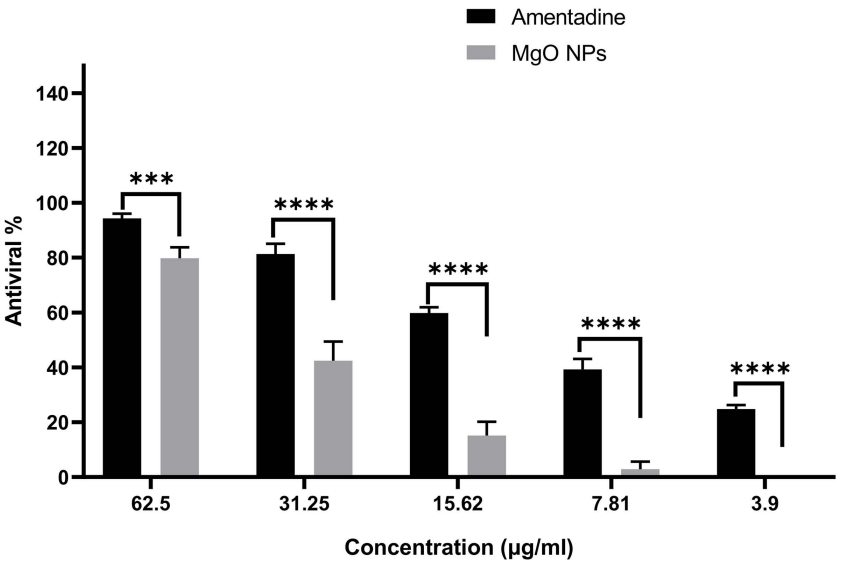

Fig 12. Antiviral efficacy of bio_synthesized MgONPs against HAV.

https://doi.org/10.1371/journal.pone.0332367.g012

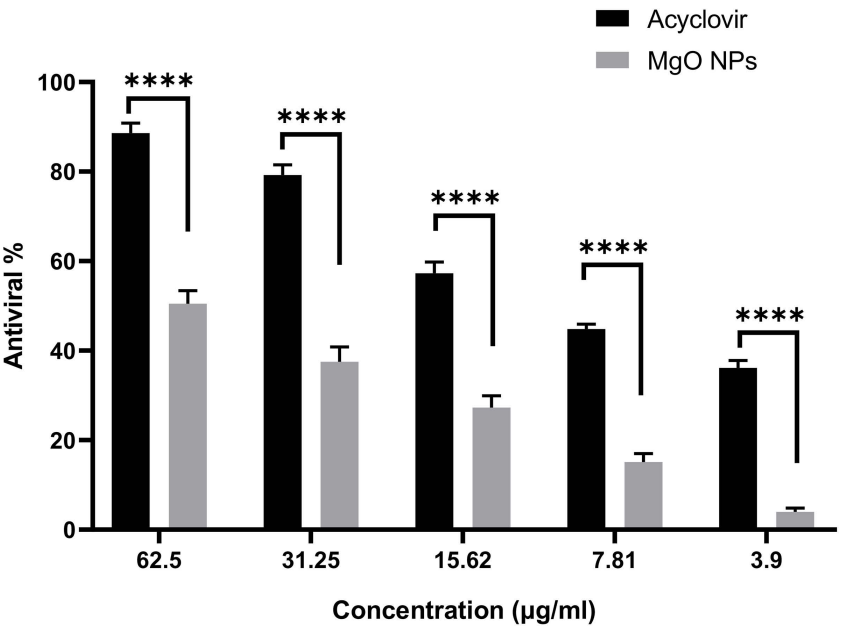

Fig 13. Antiviral efficacy of bio_synthesized MgONPs against HSV1.

https://doi.org/10.1371/journal.pone.0332367.g013

down or deactivate viral particles [67]. For example, they can break the disulfide bonds that keep viruses structural, or they can release metal ions which combine with viral protective envelopes to produce ROS that harm viruses' vital biological macromolecules like proteins and nucleic acids [90]. Furthermore, infected cells may create ROS in response to NP exposure. These ROS can damage viral proteins, DNA, and lipid membranes, which eventually prevents the virus from

replicating and infecting new cells [91]. Certain authors have found that coating substances, such flavonoids, alkaloids, and terpenoids, that increase their antiviral properties can impact the antiviral effects of green-produced NPs [92,93].

Conclusion

For the first time, WP extract was utilized in the eco-friendly synthesis of MgO-NPs production. The average size range of 6–17 nm. This green approach is environmentally safe, as it avoided hazardous chemicals and high-energy processes. The biosynthesized MgO-NPs demonstrated significant antibiofilm, antioxidant, and antibacterial action against tested bacteria as well as the unicellular fungal pathogen *C. albicans*. Additionally, at acceptable doses, MgO-NPs exhibit antiviral efficacy against HAV and HSV1. The enzyme hybrid MgO-NPs complex is stable, as demonstrated by the docking simulation of MgO-NPs, and the DHFR may be a potential mechanism of action. MgO-NPs represent a promising therapeutic candidate, pending further in vivo validation.

Supporting information

S1 File. Antimicrobial activity of MgO-NPs at 1000 µg/mL.
(PDF)

S2 File. Anti-biofilm assay of MgO-NPs.
(PDF)

S3 File. Antioxidant assay of MgONPs.
(PDF)

S4 File. Antiviral activity of MgONPs against HSV1 and HAV viruses.
(PDF)

Author contributions

Conceptualization: Mohamed K.Y. Soliman, Salem S. Salem.

Data curation: Mohamed K.Y. Soliman, Mohammed S. Almuhayawi, Mohammed H. Alruhaili, Hattan S. Gattan, Amna A. Saddiq, Salem S. Salem.

Formal analysis: Mohamed K.Y. Soliman, Nashwa Hagagy, Ashwag J. Alzahrani, Soad K. Al Jaouni, Salem S. Salem.

Funding acquisition: Samy Selim, Mohammed S. Almuhayawi, Mohammed H. Alruhaili, Hattan S. Gattan, Amna A. Saddiq, Nashwa Hagagy, Ashwag J. Alzahrani, Soad K. Al Jaouni.

Investigation: Samy Selim, Mohamed K.Y. Soliman, Salem S. Salem.

Methodology: Mohamed K.Y. Soliman, Salem S. Salem.

Validation: Samy Selim, Mohamed K.Y. Soliman, Mohammed S. Almuhayawi, Mohammed H. Alruhaili, Soad K. Al Jaouni, Salem S. Salem.

Writing – original draft: Samy Selim, Mohamed K.Y. Soliman, Salem S. Salem.

Writing – review & editing: Mohamed K.Y. Soliman, Mohammed S. Almuhayawi, Mohammed H. Alruhaili, Hattan S. Gattan, Amna A. Saddiq, Nashwa Hagagy, Ashwag J. Alzahrani, Soad K. Al Jaouni, Salem S. Salem.

References

1. Singh NB, Kumar B, Usman UL, Susan MdABH. Nano revolution: exploring the frontiers of nanomaterials in science, technology, and society. Nano Struct Nano Objects. 2024;39:101299. https://doi.org/10.1016/j.nanoso.2024.101299

2. Acharya B, Behera A, Behera S, Moharana S. Recent advances in nanotechnology-based drug delivery systems for the diagnosis and treatment of reproductive disorders. ACS Appl Bio Mater. 2024;7(3):1336–61. https://doi.org/10.1021/acsabm.3c01064 PMID: 38412066
3. Kirubakaran D, Wahid JBA, Karmegam N, Jeevika R, Sellapillai L, Rajkumar M, et al. A comprehensive review on the green synthesis of nanoparticles: advancements in biomedical and environmental applications. Biomed Mater Devices. 2025. https://doi.org/10.1007/s44174-025-00295-4
4. Salem SS. A mini review on green nanotechnology and its development in biological effects. Arch Microbiol. 2023;205(4):128. https://doi.org/10.1007/s00203-023-03467-2 PMID: 36944830
5. Rana A, Yadav K, Jagadevan S. A comprehensive review on green synthesis of nature-inspired metal nanoparticles: Mechanism, application and toxicity. J Clean Production. 2020;272:122880. https://doi.org/10.1016/j.jclepro.2020.122880
6. Shiraz M, Imtiaz H, Azam A, Hayat S. Phytogenic nanoparticles: synthesis, characterization, and their roles in physiology and biochemistry of plants. Biometals. 2024;37(1):23–70. https://doi.org/10.1007/s10534-023-00542-5 PMID: 37914858
7. Salem SS, Hammad EN, Mohamed AA, El-Dougdoug W. A comprehensive review of nanomaterials: types, synthesis, characterization, and applications. Biointerface Res Appl Chem. 2022;13(1):41. https://doi.org/10.33263/briac131.041
8. Madani M, Hosny S, Alshangiti DM, Nady N, Alkhursani SA, Alkhaldi H, et al. Green synthesis of nanoparticles for varied applications: Green renewable resources and energy-efficient synthetic routes. Nanotechnol Rev. 2022;11(1):731–59. https://doi.org/10.1515/ntrev-2022-0034
9. Salem SS. Bio-fabrication of selenium nanoparticles using baker's yeast extract and its antimicrobial efficacy on food borne pathogens. Appl Biochem Biotechnol. 2022;194(5):1898–910. https://doi.org/10.1007/s12010-022-03809-8 PMID: 34994951
10. Selim S, Salem SS, Owda ME, Almuhayawi MS, Gattan HS, Alruhaili MH, et al. Biosynthesized zinc oxide nanoparticles: Multifunctional potential applications in anticancer, antibacterial, and B. subtilis DNA gyrase docking. Green Process Synthesis. 2025;14(1). https://doi.org/10.1515/gps-2024-0218
11. Suliman AA, El-Dewiny CY, Soliman MKY, Salem SS. Investigation of the effects of applying bio-magnesium oxide nanoparticle fertilizer to moringa oleifera plants on the chemical and vegetative properties of the plants' leaves. Biotechnol J. 2025;20(3):e202400536. https://doi.org/10.1002/biot.202400536 PMID: 40059570
12. Malaikozhundan B, Mohandoss S, Krishnamoorthi R, Bharathi PV, Palanisamy S, Vinodhini J. Enhanced bactericidal, antibiofilm and antioxidative response of Lawsonia inermis leaf extract synthesized ZnO NPs loaded with commercial antibiotic. Bioprocess Biosyst Eng. 2024;47(8):1241–57. https://doi.org/10.1007/s00449-024-03000-9 PMID: 38607416
13. Vinothini P, Malaikozhundan B, Krishnamoorthi R, Dayana Senthamarai M, Shanthi D. Potential inhibition of biofilm forming bacteria and fungi and DPPH free radicals using Tamarindus indica fruit extract assisted iron oxide nanoparticle. Inorganic Chem Commun. 2023;156:111206. https://doi.org/10.1016/j.inoche.2023.111206
14. Soliman MKY, Amin MAA, Nowwar AI, Hendy MH, Salem SS. Green synthesis of selenium nanoparticles from Cassia javanica flowers extract and their medical and agricultural applications. Sci Reports. 2024;14(1). https://doi.org/10.1038/s41598-024-77353-2
15. Gad ES, Salem SS, Selim S, Almuhayawi MS, Alruhaili MH, Al Jaouni SK, et al. A comprehensive study on characterization of biosynthesized copper-oxide nanoparticles, their capabilities as anticancer and antibacterial agents, and predicting optimal docking poses into the cavity of S. aureus DHFR. PLoS One. 2025;20(4):e0319791. https://doi.org/10.1371/journal.pone.0319791 PMID: 40168419
16. Shah M, Fawcett D, Sharma S, Tripathy SK, Poinern GEJ. Green synthesis of metallic nanoparticles via biological entities. Materials (Basel). 2015;8(11):7278–308. https://doi.org/10.3390/ma8115377 PMID: 28793638
17. Salem SS, Fouda A. Green synthesis of metallic nanoparticles and their prospective biotechnological applications: an overview. Biol Trace Elem Res. 2021;199(1):344–70. https://doi.org/10.1007/s12011-020-02138-3 PMID: 32377944
18. Amina M, Al Musayeib NM, Alarfaj NA, El-Tohamy MF, Oraby HF, Al Hamoud GA, et al. Biogenic green synthesis of MgO nanoparticles using Saussurea costus biomasses for a comprehensive detection of their antimicrobial, cytotoxicity against MCF-7 breast cancer cells and photocatalysis potentials. PLoS One. 2020;15(8):e0237567. https://doi.org/10.1371/journal.pone.0237567 PMID: 32797097
19. Abdel-Aziz MM, Emam TM, Elsherbiny EA. Bioactivity of magnesium oxide nanoparticles synthesized from cell filtrate of endobacterium Burkholderia rinojensis against Fusarium oxysporum. Mater Sci Eng C Mater Biol Appl. 2020;109:110617. https://doi.org/10.1016/j.msec.2019.110617 PMID: 32229008
20. Malaikozhundan B, Vaseeharan B, Vijayakumar S, Pandiselvi K, Kalanjiam MAR, Murugan K, et al. Biological therapeutics of Pongamia pinnata coated zinc oxide nanoparticles against clinically important pathogenic bacteria, fungi and MCF-7 breast cancer cells. Microb Pathog. 2017;104:268–77. https://doi.org/10.1016/j.micpath.2017.01.029 PMID: 28115262
21. Pugazhendhi A, Prabhu R, Muruganantham K, Shanmuganathan R, Natarajan S. Anticancer, antimicrobial and photocatalytic activities of green synthesized magnesium oxide nanoparticles (MgONPs) using aqueous extract of Sargassum wightii. J Photochem Photobiol B. 2019;190:86–97. https://doi.org/10.1016/j.jphotobiol.2018.11.014 PMID: 30504053
22. Krishnamoorthy K, Moon JY, Hyun HB, Cho SK, Kim S-J. Mechanistic investigation on the toxicity of MgO nanoparticles toward cancer cells. J Mater Chem. 2012;22(47):24610. https://doi.org/10.1039/c2jm35087d
23. Vijai Anand K, Anugraga AR, Kannan M, Singaravelu G, Govindaraju K. Bio-engineered magnesium oxide nanoparticles as nano-priming agent for enhancing seed germination and seedling vigour of green gram (Vigna radiata L.). Materials Letters. 2020;271:127792. https://doi.org/10.1016/j.matlet.2020.127792

24. Verma SK, Nisha K, Panda PK, Patel P, Kumari P, Mallick MA, et al. Green synthesized MgO nanoparticles infer biocompatibility by reducing in vivo molecular nanotoxicity in embryonic zebrafish through arginine interaction elicited apoptosis. Sci Total Environ. 2020;713:136521. https://doi.org/10.1016/j.scitotenv.2020.136521 PMID: 31951838
25. Abdelfattah NAH, Yousef MA, Badawy AA, Salem SS. Influence of biosynthesized magnesium oxide nanoparticles on growth and physiological aspects of cowpea (Vigna unguiculata L.) plant, cowpea beetle, and cytotoxicity. Biotechnol J. 2023;18(12):e2300301. https://doi.org/10.1002/biot.202300301 PMID: 37615241
26. Franco Castillo I, García Guillén E, M de la Fuente J, Silva F, Mitchell SG. Preventing fungal growth on heritage paper with antifungal and cellulase inhibiting magnesium oxide nanoparticles. J Mater Chem B. 2019;7(41):6412–9. https://doi.org/10.1039/c9tb00992b PMID: 31642855
27. Maji J, Pandey S, Basu S. Synthesis and evaluation of antibacterial properties of magnesium oxide nanoparticles. Bull Mater Sci. 2019;43(1). https://doi.org/10.1007/s12034-019-1963-5
28. Moeini-Nodeh S, Rahimifard M, Baeeri M, Abdollahi M. Functional Improvement in rats' pancreatic islets using magnesium oxide nanoparticles through antiapoptotic and antioxidant pathways. Biol Trace Elem Res. 2017;175(1):146–55. https://doi.org/10.1007/s12011-016-0754-8 PMID: 27234250
29. Manikandan S, Vickram S, Sirohi R, Subbaiya R, Krishnan RY, Karmegam N, et al. Critical review of biochemical pathways to transformation of waste and biomass into bioenergy. Bioresour Technol. 2023;372:128679. https://doi.org/10.1016/j.biortech.2023.128679 PMID: 36706818
30. Thanigaivel S, Vickram S, Manikandan S, Deena SR, Subbaiya R, Karmegam N, et al. Sustainability and carbon neutralization trends in microalgae bioenergy production from wastewater treatment: A review. Bioresour Technol. 2022;364:128057. https://doi.org/10.1016/j.biortech.2022.128057 PMID: 36195218
31. Deena SR, Vickram AS, Manikandan S, Subbaiya R, Karmegam N, Ravindran B, et al. Enhanced biogas production from food waste and activated sludge using advanced techniques - A review. Bioresour Technol. 2022;355:127234. https://doi.org/10.1016/j.biortech.2022.127234 PMID: 35489575
32. Ghotekar S. A review on plant extract mediated biogenic synthesis of CdO nanoparticles and their recent applications. Asian J Green Chem. 2019;3(2):187–200.
33. Hashem AH, El-Sayyad GS, Al-Askar AA, Marey SA, AbdElgawad H, Abd-Elsalam KA, et al. Watermelon rind mediated biosynthesis of bimetallic selenium-silver nanoparticles: characterization, antimicrobial and anticancer activities. Plants (Basel). 2023;12(18):3288. https://doi.org/10.3390/plants12183288 PMID: 37765453
34. Sharma G, Soni R, Jasuja ND. Phytoassisted synthesis of magnesium oxide nanoparticles with Swertia chirayaita. J Taibah Univ Sci. 2017;11(3):471–7. https://doi.org/10.1016/j.jtusci.2016.09.004
35. Ali S, Sudha KG, Karunakaran G, Kowsalya M, Kolesnikov E, Gorshenkov MV, et al. Novel Leea grandifolia leaves mediated synthesis of ZnO nanorods for photocatalytic and anticancer applications. Appl Organometallic Chem. 2021;35(7):e6239.
36. Soliman MKY, Salem SS, Abu-Elghait M, Azab MS. Biosynthesis of silver and gold nanoparticles and their efficacy towards antibacterial, antibiofilm, cytotoxicity, and antioxidant activities. Appl Biochem Biotechnol. 2023;195(2):1158–83. https://doi.org/10.1007/s12010-022-04199-7 PMID: 36342621
37. Gawade VV, Gavade NL, Shinde HM, Babar SB, Kadam AN, Garadkar KM. Green synthesis of ZnO nanoparticles by using Calotropis procera leaves for the photodegradation of methyl orange. J Mater Sci. 2017;28(18):14033–9. https://doi.org/10.1007/s10854-017-7254-2
38. Shawky M, Suleiman WB, Farrag AA. Antibacterial resistance pattern in clinical and non-clinical bacteria by phenotypic and genotypic assessment. J Pure Appl Microbiol. 2021;15(4):2270–9. https://doi.org/10.22207/jpam.15.4.49
39. Patel J, Weinstein M, Eliopoulos G, Jenkins S, Lewis J, Limbago B. M100 performance standards for antimicrobial susceptibility testing. United States: Clinical and Laboratory Standards Institute; 2017.
40. Abbey TC, Deak E. What's new from the CLSI subcommittee on antimicrobial susceptibility testing M100, 29th Edition. Clin Microbiol Newslett. 2019;41(23):203–9. https://doi.org/10.1016/j.clinmicnews.2019.11.002
41. Soliman MKY, Abu-Elghait M, Salem SS, Azab MS. Multifunctional properties of silver and gold nanoparticles synthesis by Fusarium pseudonygamai. Biomass Conv Bioref. 2022;14(22):28253–70. https://doi.org/10.1007/s13399-022-03507-9
42. Basseem M, Emam AA, Kamal FH, Gamal AM, Abo Faraha SA. Photocatalytic activity of co-doped NPs based on ZnO as a new class of antimicrobial agents: synthesis, characterization, kinetics, isotherm, and in silico molecular docking simulation. Appl Organom Chemis. 2023;37(10). https://doi.org/10.1002/aoc.7238
43. Yildirim A, Mavi A, Kara AA. Determination of antioxidant and antimicrobial activities of Rumex crispus L. extracts. J Agric Food Chem. 2001;49(8):4083–9. https://doi.org/10.1021/jf0103572 PMID: 11513714
44. Almuhayawi MS, Alruhaili MH, Soliman MKY, Tarabulsi MK, Ashy RA, Saddiq AA, et al. Investigating the in vitro antibacterial, antibiofilm, antioxidant, anticancer and antiviral activities of zinc oxide nanoparticles biofabricated from Cassia javanica. PLoS One. 2024;19(10):e0310927. https://doi.org/10.1371/journal.pone.0310927 PMID: 39352889
45. Ratan ZA, Mashrur FR, Chhoan AP, Shahriar SM, Haidere MF, Runa NJ, et al. Silver nanoparticles as potential antiviral agents. Pharmaceutics. 2021;13(12):2034. https://doi.org/10.3390/pharmaceutics13122034 PMID: 34959320
46. Adeyemi JO, Oriola AO, Onwudiwe DC, Oyedeji AO. Plant extracts mediated metal-based nanoparticles: synthesis and biological applications. Biomolecules. 2022;12(5):627. https://doi.org/10.3390/biom12050627 PMID: 35625555

47. Nadaf SJ, Jadhav NR, Naikwadi HS, Savekar PL, Sapkal ID, Kambli MM, et al. Green synthesis of gold and silver nanoparticles: updates on research, patents, and future prospects. OpenNano. 2022;8:100076. https://doi.org/10.1016/j.onano.2022.100076
48. Ringe E. Shapes, plasmonic properties, and reactivity of magnesium nanoparticles. J Phys Chem C Nanomater Interfaces. 2020;124(29):15665–79. https://doi.org/10.1021/acs.jpcc.0c03871 PMID: 32905178
49. Fedlheim DL, Foss CA. Metal nanoparticles: synthesis, characterization, and applications. CRC Press; 2001.
50. Jeevanandam J, Chan YS, Danquah MK. Biosynthesis and characterization of MgO nanoparticles from plant extracts via induced molecular nucleation. New J Chem. 2017;41(7):2800–14. https://doi.org/10.1039/c6nj03176e
51. Abdallah Y, Ogunyemi SO, Abdelazez A, Zhang M, Hong X, Ibrahim E, et al. The green synthesis of MgO nano-flowers using Rosmarinus officinalis L. (Rosemary) and the antibacterial activities against Xanthomonas oryzae pv. oryzae. Biomed Res Int. 2019;2019:5620989. https://doi.org/10.1155/2019/5620989 PMID: 30906776
52. Nguyen DTC, Dang HH, Vo D-VN, Bach LG, Nguyen TD, Tran TV. Biogenic synthesis of MgO nanoparticles from different extracts (flower, bark, leaf) of Tecoma stans (L.) and their utilization in selected organic dyes treatment. J Hazard Mater. 2021;404(Pt A):124146. https://doi.org/10.1016/j.jhazmat.2020.124146 PMID: 33053473
53. Shawky AM, El-Tohamy MF. Highly functionalized modified metal oxides polymeric sensors for potentiometric determination of letrozole in commercial oral tablets and biosamples. Polymers (Basel). 2021;13(9):1384. https://doi.org/10.3390/polym13091384 PMID: 33922800
54. Patle TK, Shrivas K, Kurrey R, Upadhyay S, Jangde R, Chauhan R. Phytochemical screening and determination of phenolics and flavonoids in Dillenia pentagyna using UV-vis and FTIR spectroscopy. Spectrochim Acta A Mol Biomol Spectrosc. 2020;242:118717. https://doi.org/10.1016/j.saa.2020.118717 PMID: 32745936
55. Subash M, Chandrasekar M, Panimalar S, Inmozhi C, Parasuraman K, Uthrakumar R, et al. Pseudo-first kinetics model of copper doping on the structural, magnetic, and photocatalytic activity of magnesium oxide nanoparticles for energy application. Biomass Conv Bioref. 2022;13(4):3427–37. https://doi.org/10.1007/s13399-022-02993-1
56. Alavi M, Karimi N. Hemoglobin self-assembly and antibacterial activities of bio-modified Ag-MgO nanocomposites by different concentrations of Artemisia haussknechtii and Protoparmeliopsis muralis extracts. Int J Biol Macromol. 2020;152:1174–85. https://doi.org/10.1016/j.ijbiomac.2019.10.207 PMID: 31760003
57. Lekota MW, Dimpe KM, Nomngongo PN. MgO-ZnO/carbon nanofiber nanocomposite as an adsorbent for ultrasound-assisted dispersive solid-phase microextraction of carbamazepine from wastewater prior to high-performance liquid chromatographic detection. J Anal Sci Technol. 2019;10(1). https://doi.org/10.1186/s40543-019-0185-1
58. Hassan SE-D, Fouda A, Saied E, Farag MMS, Eid AM, Barghoth MG, et al. Rhizopus oryzae-mediated green synthesis of Magnesium Oxide Nanoparticles (MgO-NPs): a promising tool for antimicrobial, mosquitocidal action, and tanning effluent treatment. J Fungi (Basel). 2021;7(5):372. https://doi.org/10.3390/jof7050372 PMID: 34068709
59. Ammulu MA, Vinay Viswanath K, Giduturi AK, Vemuri PK, Mangamuri U, Poda S. Phytoassisted synthesis of magnesium oxide nanoparticles from Pterocarpus marsupium rox.b heartwood extract and its biomedical applications. J Genet Eng Biotechnol. 2021;19(1):21. https://doi.org/10.1186/s43141-021-00119-0 PMID: 33507438
60. Nguyen N-YT, Grelling N, Wetteland CL, Rosario R, Liu H. Antimicrobial Activities and Mechanisms of Magnesium Oxide Nanoparticles (nMgO) against Pathogenic Bacteria, Yeasts, and Biofilms. Sci Rep. 2018;8(1):16260. https://doi.org/10.1038/s41598-018-34567-5 PMID: 30389984
61. Ali A, Zafar H, Zia M, Ul Haq I, Phull AR, Ali JS, et al. Synthesis, characterization, applications, and challenges of iron oxide nanoparticles. Nanotechnol Sci Appl. 2016;9:49–67. https://doi.org/10.2147/NSA.S99986 PMID: 27578966
62. Santhoshkumar T, Rahuman AA, Jayaseelan C, Rajakumar G, Marimuthu S, Kirthi AV, et al. Green synthesis of titanium dioxide nanoparticles using Psidium guajava extract and its antibacterial and antioxidant properties. Asian Pac J Trop Med. 2014;7(12):968–76. https://doi.org/10.1016/S1995-7645(14)60171-1 PMID: 25479626
63. Yoon JY, Yeom W, Kim H, Beuchat LR, Ryu J-H. Effects of temperature, pH and sodium chloride on antimicrobial activity of magnesium oxide nanoparticles against E. coli O157:H7. J Appl Microbiol. 2022;133(4):2474–83. https://doi.org/10.1111/jam.15719 PMID: 35894203
64. Das S, Vishakha K, Banerjee S, Nag D, Ganguli A. Tetracycline-loaded magnesium oxide nanoparticles with a potential bactericidal action against multidrug-resistant bacteria: In vitro and in vivo evidence. Colloids Surf B Biointerfaces. 2022;217:112688. https://doi.org/10.1016/j.colsurfb.2022.112688 PMID: 35841801
65. Nisar P, Ali N, Rahman L, Ali M, Shinwari ZK. Antimicrobial activities of biologically synthesized metal nanoparticles: an insight into the mechanism of action. J Biol Inorg Chem. 2019;24(7):929–41. https://doi.org/10.1007/s00775-019-01717-7 PMID: 31515623
66. Li X, Feng Y, Li H, Zhang Q. Effect of anionic groups on the antibacterial activity of magnesium oxide nanoparticles. Coll Surf A. 2022;635:127978. https://doi.org/10.1016/j.colsurfa.2021.127978
67. Bhattacharya P, Dey A, Neogi S. An insight into the mechanism of antibacterial activity by magnesium oxide nanoparticles. J Mater Chem B. 2021;9(26):5329–39. https://doi.org/10.1039/d1tb00875g PMID: 34143165
68. Sawai J, Kojima H, Igarashi H, Hashimoto A, Shoji S, Takehara A, et al. Escherichia coli damage by ceramic powder slurries. J Chem Eng Japan / JCEJ. 1997;30(6):1034–9. https://doi.org/10.1252/jcej.30.1034
69. Treccani L. Interactions between surface material and bacteria: from biofilm formation to suppression. Surface Functionalized Ceramics;2023: 283–335.

70. Vestby LK, Grønseth T, Simm R, Nesse LL. Bacterial biofilm and its role in the pathogenesis of disease. Antibiotics (Basel). 2020;9(2):59. https://doi.org/10.3390/antibiotics9020059 PMID: 32028684
71. Donlan RM. Biofilms and device-associated infections. Emerg Infect Dis. 2001;7(2):277–81. https://doi.org/10.3201/eid0702.010226 PMID: 11294723
72. Khan F, Manivasagan P, Lee J-W, Pham DTN, Oh J, Kim Y-M. Fucoidan-stabilized gold nanoparticle-mediated biofilm inhibition, attenuation of virulence and motility properties in pseudomonas aeruginosa PAO1. Mar Drugs. 2019;17(4):208. https://doi.org/10.3390/md17040208 PMID: 30987163
73. Ramezani Farani M, Farsadrooh M, Zare I, Gholami A, Akhavan O. Green synthesis of magnesium oxide nanoparticles and nanocomposites for photocatalytic antimicrobial, antibiofilm and antifungal applications. Catalysts. 2023;13(4):642. https://doi.org/10.3390/catal13040642
74. Younis IY, El-Hawary SS, Eldahshan OA, Abdel-Aziz MM, Ali ZY. Green synthesis of magnesium nanoparticles mediated from Rosa floribunda charisma extract and its antioxidant, antiaging and antibiofilm activities. Sci Rep. 2021;11(1):16868. https://doi.org/10.1038/s41598-021-96377-6 PMID: 34413416
75. Hayat S, Muzammil S, Rasool MH, Nisar Z, Hussain SZ, Sabri AN, et al. In vitro antibiofilm and anti-adhesion effects of magnesium oxide nanoparticles against antibiotic resistant bacteria. Microbiol Immunol. 2018;62(4):211–20. https://doi.org/10.1111/1348-0421.12580 PMID: 29405384
76. Wong CW, Chan YS, Jeevanandam J, Pal K, Bechelany M, Abd Elkodous M, et al. Response surface methodology optimization of monodispersed MgO nanoparticles fabricated by ultrasonic-assisted Sol–Gel method for outstanding antimicrobial and antibiofilm activities. J Clust Sci. 2019;31(2):367–89. https://doi.org/10.1007/s10876-019-01651-3
77. Makhluf S, Dror R, Nitzan Y, Abramovich Y, Jelinek R, Gedanken A. Microwave-assisted synthesis of nanocrystalline MgO and its use as a bacteriocide. Adv Funct Materials. 2005;15(10):1708–15. https://doi.org/10.1002/adfm.200500029
78. Naqvi AAT, Mohammad T, Hasan GM, Hassan MI. Advancements in docking and molecular dynamics simulations towards ligand-receptor interactions and structure-function relationships. Curr Top Med Chem. 2018;18(20):1755–68. https://doi.org/10.2174/1568026618666181025114157 PMID: 30360721
79. Shahzadi I, Islam M, Saeed H, Haider A, Shahzadi A, Haider J, et al. Formation of biocompatible MgO/cellulose grafted hydrogel for efficient bactericidal and controlled release of doxorubicin. Int J Biol Macromol. 2022;220:1277–86. https://doi.org/10.1016/j.ijbiomac.2022.08.142 PMID: 36030978
80. Orshiso TA, Zereffa EA, Murthy HCA, Demissie TB, Ghotekar S, Pagar K, et al. One-pot biopreparation of trimetallic ZnO–MgO–CuO nanoparticles: enhanced cytotoxicity, antibacterial activities and molecular docking studies. Chem Af. 2024;7(4):1963–80. https://doi.org/10.1007/s42250-023-00830-0
81. Jahan IA, Hossain MH, Ahmed KS, Sultana Z, Biswas PK, Nada K. Antioxidant activity of Moringa oleifera seed extracts. Orient Pharm Exp Med. 2018;18(4):299–307. https://doi.org/10.1007/s13596-018-0333-y
82. Sanmugapriya E, Venkataraman S. Studies on hepatoprotective and antioxidant actions of Strychnos potatorum Linn. seeds on CCl4-induced acute hepatic injury in experimental rats. J Ethnopharmacol. 2006;105(1–2):154–60. https://doi.org/10.1016/j.jep.2005.10.028 PMID: 16388923
83. John Sushma N, Prathyusha D, Swathi G, Madhavi T, Deva Prasad Raju B, Mallikarjuna K, et al. Facile approach to synthesize magnesium oxide nanoparticles by using Clitoria ternatea—characterization and in vitro antioxidant studies. Appl Nanosci. 2015;6(3):437–44. https://doi.org/10.1007/s13204-015-0455-1
84. Dobrucka R. Synthesis of MgO nanoparticles using artemisia abrotanum herba extract and their antioxidant and photocatalytic properties. Iran J Sci Technol Trans Sci. 2016;42(2):547–55. https://doi.org/10.1007/s40995-016-0076-x
85. Qing Y, Cheng L, Li R, Liu G, Zhang Y, Tang X, et al. Potential antibacterial mechanism of silver nanoparticles and the optimization of orthopedic implants by advanced modification technologies. Int J Nanomedicine. 2018;13:3311–27. https://doi.org/10.2147/IJN.S165125 PMID: 29892194
86. Lloyd RV, Hanna PM, Mason RP. The origin of the hydroxyl radical oxygen in the Fenton reaction. Free Radic Biol Med. 1997;22(5):885–8. https://doi.org/10.1016/s0891-5849(96)00432-7 PMID: 9119257
87. Stohs SJ, Bagchi D. Oxidative mechanisms in the toxicity of metal ions. Free Radic Biol Med. 1995;18(2):321–36. https://doi.org/10.1016/0891-5849(94)00159-h PMID: 7744317
88. Dizdaroglu M, Jaruga P. Mechanisms of free radical-induced damage to DNA. Free Radic Res. 2012;46(4):382–419. https://doi.org/10.3109/10715762.2011.653969 PMID: 22276778
89. Kaur H, Kumar S, Bouzid G. Exploring the role of different phytochemicals on the morphological variations of metal and metal oxide nanomaterials for biomedical application. Interactions. 2024;245(1). https://doi.org/10.1007/s10751-024-02088-5
90. Sakudo A, Yamashiro R, Haritani M, Furusaki K, Onishi R, Onodera T. Inactivation of non-enveloped viruses and bacteria by an electrically charged disinfectant containing meso-structure nanoparticles via modification of the genome. Int J Nanomedicine. 2020;15:1387–95. https://doi.org/10.2147/IJN.S229880 PMID: 32184593
91. Luceri A, Francese R, Lembo D, Ferraris M, Balagna C. Silver nanoparticles: review of antiviral properties, mechanism of action and applications. Microorganisms. 2023;11(3):629. https://doi.org/10.3390/microorganisms11030629 PMID: 36985203
92. Kamli MR, Srivastava V, Hajrah NH, Sabir JSM, Ali A, Malik MA, et al. Phytogenic fabrication of Ag-Fe bimetallic nanoparticles for cell cycle arrest and apoptosis signaling pathways in candida auris by generating oxidative stress. Antioxidants (Basel). 2021;10(2):182. https://doi.org/10.3390/antiox10020182 PMID: 33513888
93. Elnosary ME, Aboelmagd HA, Sofy AR, Hmed AA, Refaey EE, Ali SM, et al. Uncovering and evaluating coconut oil-loaded silica nanoemulsion as anti-viral, bacterial, and fungal: synthesis, fabrication, characterization, and biosafety profiles. Beni-Suef Univ J Basic Appl Sci. 2024;13(1). https://doi.org/10.1186/s43088-024-00513-w